arXiv:cond-mat/0209648v2 [cond-mat.str-el] 6 Feb 2003

Effect of a magnetic field on long-range magnetic order in stage-4 and stage-6 superconducting La_2CuO_{4+y}

B. Khaykovich,[1] R. J. Birgeneau,[2] F. C. Chou,[1] R. W. Erwin,[3] M. A. Kastner,[1]
S.-H. Lee,[3] Y. S. Lee,[1] P. Smeibidl,[4] P. Vorderwisch,[4] and S. Wakimoto[2]

[1]*Department of Physics and Center for Material Science and Engineering, Massachusetts Institute of Technology, Cambridge, MA 02139*
[2]*Department of Physics, University of Toronto, Toronto, Ontario M5S 1A7, Canada*
[3]*Center for Neutron Research, NIST, Gaithersburg, MD 20899-8562*
[4]*4 BENSC, Hahn-Meitner Institute, D-14109 Berlin, Germany*

(Dated: March 22, 2022)

We have measured the enhancement of the static incommensurate spin-density wave (SDW) order by an applied magnetic field in stage-4 and stage-6 samples of superconducting La_2CuO_{4+y}. We show that the stage-6 La_2CuO_{4+y} (T_c=32 K) forms static long-range SDW order with the same wave-vector as that in the previously studied stage-4 material. We have measured the field dependence of the SDW magnetic Bragg peaks in both stage-4 and stage-6 materials at fields up to 14.5 T. A recent model of competing SDW order and superconductivity describes these data well.

PACS numbers: 74.72.Dn, 75.25.+z, 75.30.Fv, 75.50.Ee

High-transition-temperature superconductors made by doping La_2CuO_4 have a very rich magnetic phase diagram as a function of dopant concentration and the nature of the dopants. In particular, neutron scattering experiments first demonstrated incommensurate dynamic spin correlations in $La_{2-x}Sr_xCuO_4$ for a wide range of x.[1,2] Later, static incommensurate spin-density wave (SDW) order was discovered in superconducting $(La_{2-y-x}Nd_y)Sr_xCuO_4$, $La_{2-x}Sr_xCuO_4$ at $x \approx 1/8$, and La_2CuO_{4+y},[3,4,5] as well as in insulating $La_{2-x}Sr_xCuO_4$, $0.02 \leq x \leq 0.05$.[6] These observations stimulated many experimental and theoretical studies of the nature of the magnetic correlations and the static SDW order and their interaction with superconductivity (SC) in doped La_2CuO_4 and other cuprate superconductors.

In our recent neutron scattering experiments on excess-oxygen-doped La_2CuO_{4+y} we have shown that an applied magnetic field serves as a weak perturbation helping to probe the nature of this interaction.[7] The results of Ref. 7, combined with similar results on $La_{2-x}Sr_xCuO_4$ for $x = 0.12$,[8] 0.16[9] and 0.10,[10] together with recent theoretical studies,[11,12,13] have led to a consistent picture of microscopic coexistence and competition between SC and SDW orders. Experimentally, the SDW signal increases when the field is applied below the superconducting T_c. This occurs because the SC order parameter is suppressed in the presence of a magnetic field, and as a result, the competing SDW order is enhanced.[11,14] Additional evidence that it is the microscopic interaction between SC and SDW order that drives the enhancement of the SDW peak intensity comes from recent experiments on lightly-doped non-superconducting $La_{2-x}Sr_xCuO_4$. There, an applied field actually *suppresses* the static incommensurate SDW order, in contrast to the behavior observed in the SC samples.[15]

Although there is good qualitative agreement between our previous experimental results[7] and theory,[11] a quantitative comparison has been difficult to make. This is primarily because the previous measurements have been limited to fields below 9 T and by the availability of samples of only one doping.

Therefore, we have expanded our magnetic field studies of superconducting La_2CuO_{4+y} in two directions. First, we have applied higher magnetic fields in order to test the predicted field dependence of the SDW peak intensity. Second, we have measured the effect of an applied field on two samples of different doping, a predominantly stage-6 sample (Sample 1) with $T_c = 32$ K and a stage-4 sample (Sample 2) with $T_c = 42$ K. Magnetic properties of this crystal have been reported in Ref. 7, where it is also called Sample 2. We find that the stage-6 sample exhibits static SDW order similar to that of the stage-4 sample. We also find that the field dependence of the SDW Bragg peak intensity, predicted by Demler *et al.*,[11] describes our results for both samples quite well. This is especially clear for the stage-4 sample.

There is a significant difference, however, in the relative increase of the magnetic signal with field for the two samples. We interpret the difference as arising from different volume fractions that are ordered magnetically. Based on μSR measurements,[16,17] it has been argued that the SDW and SC order parameters are not microscopically homogeneous throughout the sample, but that small regions of fully developed static magnetic moment percolate, leading to long-range magnetic order. It is thus hypothesized that the enhancement of the static magnetism in an applied field comes primarily from regions where the SDW order is weak. Therefore, any change in the SDW signal must depend of the volume fraction of the magnetically ordered phase at zero field.[7,16,17]

Single crystals of La_2CuO_4 have been grown by the travelling solvent floating zone technique and subsequently oxidized in an electrochemical cell, as described previously.[5] Sample 2 is prepared by oxidation at room temperature, while Sample 1 is oxidized at 50 °C. SQUID magnetization measurements have been made on a small

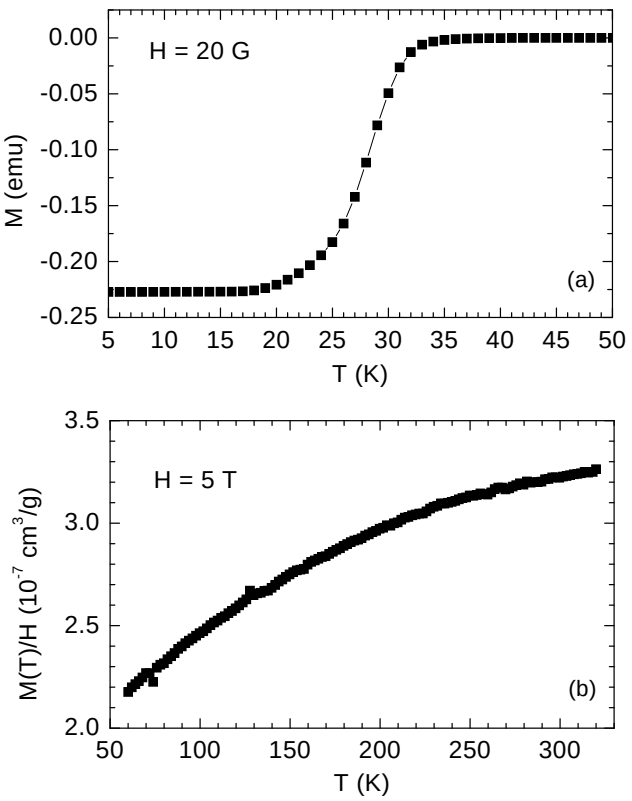


FIG. 1: Temperature dependence of the magnetization of a small piece of Sample 1. (a) Magnetization showing the onset of superconductivity, H = 20 G. (b) Susceptibility showing the absence of the weak ferromagnetism, H = 5 T. Similar measurements for Sample 2 may be found in Ref. 7

piece of each of the two samples used for the neutron measurements. For Sample 2 (stage-4) the magnetization studies evince a sharp single transition to the SC state at $T_c = 42$ K (onset). For Sample 1 (stage-6), a slightly rounded transition at 32 K (decrease by 10%) is found. The magnetization of Sample 1 is shown in the Fig. 1a. Magnetization studies also reveal the absence of weak ferromagnetism, indicating little if any remnant undoped La_2CuO_4. This is shown in Fig. 1b for Sample 1; similar data for Sample 2 have been published earlier.[7]

Neutron scattering measurements were made on the two crystals, Sample 1 of 2.9 grams and Sample 2 of 2.6 grams in mass. Our previously reported measurements of staging behavior, SDW order,[5] and the effect of magnetic field[7] were made using Sample 2 in magnetic fields up to 7 T. Elastic neutron scattering studies were performed at the NIST Center for Neutron Research in Gaithersburg, MD and at the Hahn-Meitner Institute (HMI), Berlin, Germany. We used the BT7 thermal triple-axis spectrometer at NIST, with an incident neutron energy of 13.4 meV, to measure the stage-order of interstitial oxygen in the Sample 1. High magnetic field measurements were done on the FLEX cold-neutron triple-axis spectrometer at HMI with an incident neutron energy of 5 meV. A pyrolytic graphite (PG) monochromator and a PG analyzer were used, as well as a PG (for 13.4 meV neutrons) or cold Be (for 5 meV neutrons) filter to remove higher energy contamination from the incident neutron beam. The magnetic field was applied using a 14.5 T split-coil superconducting magnet.

The crystal structure of La_2CuO_4 is orthorhombic, space group *Bmab*. The orthorhombicity results from a slight tilt of the CuO_6 octahedra. We therefore use the orthorhombic unit cell notation with the *a*- and *b*-axes along the diagonals of the CuO_2 squares and the *c*-axis perpendicular to the layers. In reciprocal space the *H, K* and *L* axes are parallel to the *a,b*, and *c*-axes, respectively. Excess oxygen in La_2CuO_{4+y} is intercalated between the CuO_2 planes, resulting in a mass-density-wave modulation of the intercalated oxygen density along the *c*-axis. The tilt angle of the CuO_6 octahedra changes sign across the planes of maximum oxygen density, so the tilt reversal occurs every *n*th CuO_2 layer. The sample with tilt reversal every *n*th layer is called stage-*n*.[5,18] The tilt reversals of the CuO_6 octahedra result in structural Bragg peaks displaced along the *L* axis in reciprocal space by $1/n$ from the superlattice Bragg peak. Because of the staging order, the oxygen doping can not be changed continuously, and there are miscibility gaps between the lightly doped antiferromagnet, stage-6, and stage-4 phases.[18] Samples often consist of a mixture of two or more staged phases.

Fig. 2 shows elastic neutron scattering data from the Sample 1, scanned around the (0,1,4) position in reciprocal space. The pair of stage-6 peaks $(0,1,4 \pm 1/6)$ is the strongest, but the stage-4 peaks at $(0,1,4 \pm 1/4)$ are also present and correspond to 20% of the total intensity of the staging peaks. The (0,1,4) central peak arises from lightly doped La_2CuO_4 inclusions. In lightly doped samples, this structural Bragg peak arises from three-dimensional ordering of the CuO_6 octahedra tilts. The intensity of this peak is several orders of magnitude smaller than that for an undoped La_2CuO_4 sample of similar size, implying that the undoped fraction is very small. The peaks are fitted by one-dimensional Lorenzians convoluted with the instrumental resolution. The staging peaks are almost resolution-limited, corresponding to a correlation length exceeding 800 Å. We therefore conclude that this sample consists of a mixture of stage-4 and stage-6 phases, with the stage-6 phase dominant. This is in agreement with the results of magnetic susceptibility measurements, which indicate a lower $T_c = 32$ K, than a pure stage-4 sample, as noted above. Sample 2, which has been used in our previous studies, consists predominately of the stage-4 phase.[5,7]

Static long-range incommensurate SDW order has been found in the stage-4 sample below $T_m = 42$ K by neutron scattering.[5] In previous work we have shown that a magnetic field, applied perpendicular to the CuO_2 lay-

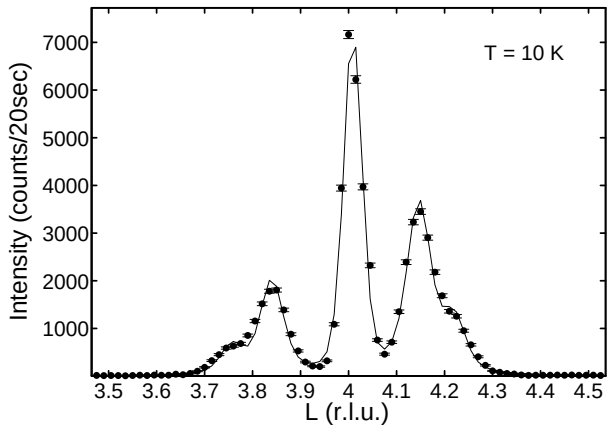


FIG. 2: Elastic scan across the staging superlattice position (0, 1, 4) at low temperatures for the stage-6 Sample 1. T = 10 K, E_i = 13.41 meV, collimation 30'-30'-S-30'-open, 3-axis mode (S denotes the sample). The fit is the result of the convolution of a one-dimensional Lorentzian with the instrumental resolution. The two pairs of peaks displaced symmetrically around the (014) position result from the staging order. The peak at (014) is the *Bmab* peak from undoped La_2CuO_4 inclusions.

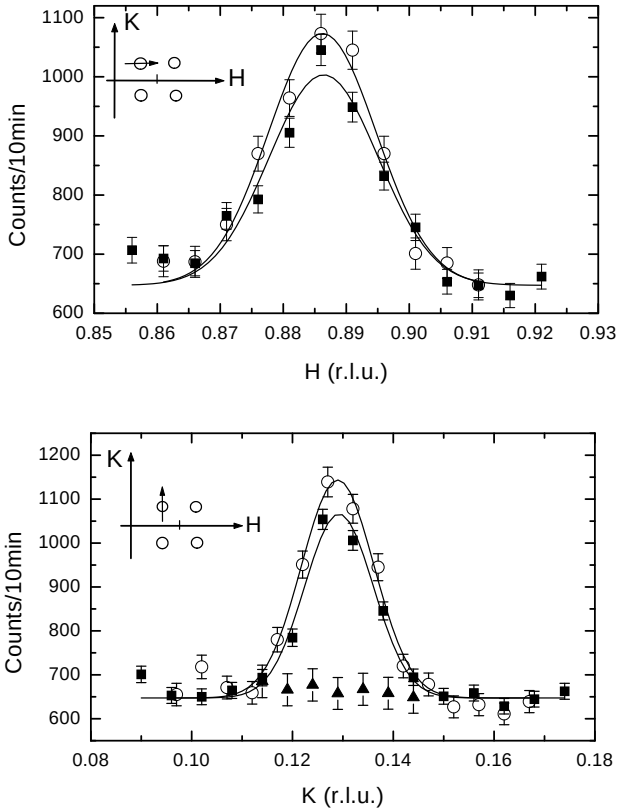


FIG. 3: Elastic scans through the incommensurate SDW Bragg peak at **Q** = (0.886, 0.129, 0) at zero applied field (squares) and H = 14.5 T (circles) for the stage-6 Sample 1. The sample is oriented such that the neutron wave vector transfer Q is parallel to the CuO_2 planes (*(H, K, 0)* in reciprocal space). The applied field is perpendicular to the CuO_2 planes. Measurements are made at T = 3 K and the background (triangles) is measured at T = 45 K. The collimation is 60'-S-60'-open, E_i = 5 meV. The inset shows schematically the positions of 4 incommensurate SDW peaks in reciprocal space together with the scan directions. The line-profile is Gaussian; the HWHM is resolution-limited.

ers, increases the intensity of the incommensurate magnetic Bragg peaks approximately linearly with field for fields up to at least 7 T. Here we find that similar behavior occurs for the stage-6 sample. Fig. 3 shows the magnetic Bragg peak resulting from the incommensurate SDW order at $H = 0$ and 14.5 T, in Sample 1. We have checked that the peak positions at $(1\pm0.114, 0\pm0.128, 0)$ are identical for both Sample 1 and Sample 2 ((1, 0, 0) is the position of the antiferromagnetic zone center for undoped La_2CuO_4). Fig. 3 clearly shows that only the intensity of the SDW peak increases with field, whereas the width and the position of the peak remain the same. The peak widths are limited by our instrument resolution, which indicates long-range magnetic order with the correlation length in excess of 400 $\AA$.

Fig. 4 shows the field dependence of the magnetic Bragg peak intensity for Sample 2 (a) and Sample 1 (b). The intensity is normalized to the zero-field value. Fig. 4(a) shows data taken both at NIST (below 7 T) and at HMI (0 T to 14.5 T). The points at 0, 3, 5 and 7 T have been measured on both spectrometers. The intensity I(H) is obtained by averaging counts from both longitudinal and transverse scans close to the peak position. The field-independent background has been measured and subtracted.

One of the most intriguing properties of stage-4 oxygen-doped La_2CuO_{4+y}, reported in Ref. 5, is that the onset of the SDW Bragg peak coincides with the superconducting T_c = 42 K. Therefore, we have measured the temperature dependence of the SDW Bragg peak for Sample 1, as shown in Fig. 5. Clearly, the SDW signal appears first at $T_m = (40 \pm 2)$ K, well above T_c = 32 K (see Fig. 1a). However, since Sample 2 contains about 20% of the stage-4 phase, this onset of the magnetic order at 40 ± 2 K may arise from the ordering of the stage-4 part alone. A closer look at the magnetization curve in Fig. 1a reveals a small drop of the magnetization at 42 K. We ascribe this to the superconducting transition of the stage-4 phase. To test whether T_c and T_m are the same for stage-6 alone, one would need a homogeneous stage-6 sample.

We now discuss these experimental results. Although Sample 1 consists of a mixture of stage-6 and stage-4 phases, the two phases must have identical SDW ordering

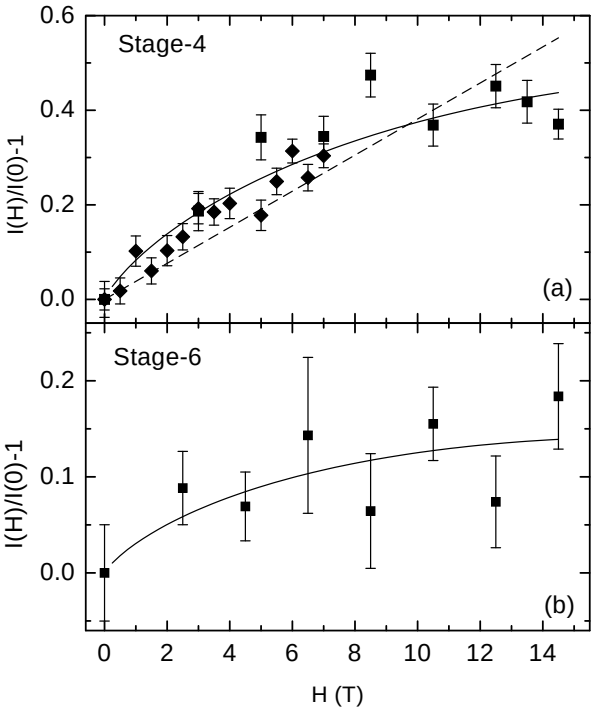


FIG. 4: Field dependence of the SDW Bragg peak intensity I(H), normalized to the zero-field intensity, I(0). (a) Sample 2, stage-4. The diamonds correspond to data taken at NIST and reported previously.[7] The squares represent the data taken at HMI. (b) Sample 1, stage-6, measured at HMI. The solid lines correspond to the function $(H/H_{c2})\ln(\theta H_{c2}/H)$ and the dashed line corresponds to a linear function H/H_{c2}, as discussed in the text. The larger error bars and smaller number of points for the HMI experiment result from limited access to the instruments.

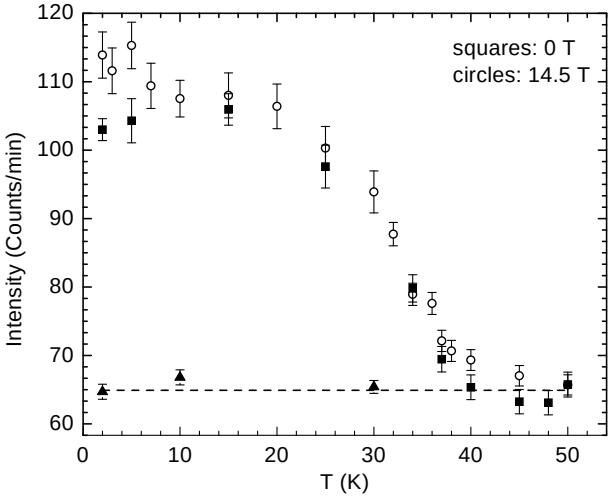


FIG. 5: Temperature dependence of the SDW Bragg peak intensity, Sample 1, stage-6. $H = 0$ T (squares) and 14.5 T (circles). The triangles correspond to the background determined by fitting SDW data, like these in Fig. 3, to a Gaussian peak plus a **Q**-independent background. At $T = 2$ K, the background comes from a scan at $H = 0$ T and at the higher temperatures from scans at $H = 14.5$ T. The dashed line is a linear fit to the background points; the background is temperature- and field-independent.

at low temperatures for the following reasons: Samples 1 and 2 are of similar size, and their incommensurate SDW peaks have intensities of (40±2) and (30±2) counts/min, respectively, at zero field. However, only 20% of Sample 1 is in the stage-4 phase. Were only the stage-4 phase magnetically ordered, the SDW peak intensity from Sample 1 would be smaller than that from Sample 2, even if 100% of the stage-4 phase were magnetically ordered. It is also important to note that the incommensurability must be identical for stage-4 and stage-6. This is evident from the sharp, resolution-limited SDW peaks. Were the peaks for stage-4 and stage-6 shifted relative to each other, a wide SDW peak would result. Finally, a pure stage-6 sample has been measured recently,[19] and this sample shows sharp SDW peaks at the same positions. Unfortunately, this pure stage-6 crystal is too small for quantitative field-dependence measurements. The single value of the incommensurability δ observed in the stage-4 and stage-6 samples may result from the saturation of δ with hole concentration. For the inelastic scattering in Sr-doped $La_{2-x}Sr_xCuO_4$, δ is equal to x for small x, but saturates above $x \simeq 0.12$.[2] The similar saturation of δ is seen for the SDW in Nd codoped samples.[3] As shown in Ref. 7, the doping of Sample 2 corresponds to a hole concentration of 0.14 per Cu, above the concentration necessary for saturation. Stage-6 samples probably also have hole concentration high enough for saturation. The incommensurability is close to the saturation value in the other La_2CuO_4-based materials. Although the saturation can thus explain quite similar values of δ in stage-4 and stage-6 samples, it is nonetheless surprising that they are identical within the experimental error of 0.002 (r.l.u.).

The model of competing order parameters[11,13] predicts the existence of three different phases: a pure SC phase, a SDW+SC phase, in which SDW order coexists with and couples to the SC order, and a pure SDW phase. The transitions between these phases occur by changing a control parameter, that is related to doping, or applied magnetic field. At zero magnetic field, stage-4 La_2CuO_{4+y} apparently resides in the SDW+SC phase. By increasing the doping, La_2CuO_{4+y} is expected to move into the pure SC phase. Unfortunately, it does

not appear to be possible to increase the doping beyond the value that gives stage-4 by additional oxidation of La_2CuO_{4+y}. (This can, of course, be accomplished by changing x in $La_{2-x}Sr_xCuO_4$[8,9,10]). When the doping decreases, La_2CuO_{4+y} is expected to remain in the SDW+SC phase, and this is confirmed by our observations.

The enhancement of the SDW order parameter in an applied field originates from the suppression of superconductivity near vortices. The superconducting order parameter $|\psi|^2$ is most strongly suppressed inside the vortex core, of radius $\xi \simeq 30$ $\AA$. But $|\psi|^2$ is also suppressed below its zero-field value even far from the cores, recovering as $(1 - 2\xi^2/r^2)$. Here ξ is the superconducting correlation length and r is the distance from the core. Since the magnetic correlation length exceeds 400 $\AA$, which is much larger than ξ, averaging $|\psi(r)|^2$ over the regions far away from the vortex is required to account for the resulting change of the SDW order parameter. The SDW peak intensity is thus predicted to increase with field as $\Delta I \sim (H/H_{c2}) \ln(\theta H_{c2}/H)$; the logarithmic correction originates from the $1/r$ term in the suppression of $|\psi|^2$. Here H_{c2} is the upper critical field of the superconductor, and θ is a constant of order unity, independent of doping.[11]

We have fitted the data in Fig. 4 using this prediction. The best fit gives $H_{c2} = 49$ T for the stage-6 Sample 1 and 67 T for the stage-4 Sample 2. In both cases θ is set to 1 for the best fit. We also show the result of a fit to a simple linear dependence, H/H_{c2}, for Sample 2 (dashed line in Fig. 4a), which describes our previous low field results adequately.[7] Clearly, the logarithmic correction to the linear dependence improves the agreement between the theoretical prediction and the data. The high field data points above 7 T are especially important in order to distinguish between the two possibilities. The "goodness-of-fit", χ^2, analysis confirms this conclusion: $\chi^2 \simeq 0.002$ is significantly smaller for the $H \ln H$ fit, than $\chi^2 \simeq 0.006$ for the linear fit.

Numerical calculations have resulted in $\theta \approx 3$ for a triangular vortex lattice.[11] Our experimental results suggest that θ is smaller, probably because the vortex lattice in La_2CuO_{4+y} is highly disordered. Further, by analogy with recent results on $La_{1.83}Sr_{0.17}CuO_4$, the vortex lattice is, in all likelihood, square rather than triangular.[20]

The upper critical fields obtained from fitting our data are in reasonable agreement with the commonly accepted values for doped La_2CuO_4-based superconductors. The applied field of 14.5 T is, therefore, much smaller than the upper critical field at T = 2 K, the temperature of the samples during the neutron scattering experiments. Therefore, the applied magnetic field acts only as a weak perturbation of the superconducting state. We have previously reported that the resistive superconducting transition of the stage-4 sample is shifted significantly to lower temperature by applied fields up to 5 T.[7] Similar measurements have not been done for the stage-6 sample, because putting electrical contacts on these heavily oxidized samples is very difficult. We point out, however, that resistance does not provide a thermodynamic measurement of the superconducting phase transition, as does, for example, the specific heat.

Fig. 4b shows the enhancement of the SDW peak intensity with field for Sample 1. The effect of applied field is much smaller for this sample, compared with the stage-4 one. The smaller change of the peak intensity may be explained by a model in which the magnetic volume fraction is less than unity, as discussed in Ref. 7. μSR measurements on a piece of Sample 2 indicate that it consists of small magnetic clusters, in which the incommensurate order has its full local moment, and that the rest of the material is non-magnetic.[16,17] Furthermore, μSR measurements indicate that the fraction that is magnetically ordered is $F \simeq 0.4$. According to the model, the superconducting order parameter is suppressed in the magnetically-ordered regions even at zero applied field. Then the enhancement of the magnetic order in the field originates from predominately non-magnetic regions, where the superconductivity is strong at zero field. Therefore, the increase in the SDW peak intensity $\Delta I \sim (1 - F)/F$. Comparing the relative increase of intensity with field for Samples 1 and 2, we conclude that about 60% of Sample 1 is magnetically ordered at zero field. μSR measurements on the stage-6 sample would serve to test this conclusion.

In conclusion, we have studied the effects of an applied magnetic field on the static incommensurate SDW order in excess-oxygen doped La_2CuO_{4+y}. We have shown that the SDW order exists in both stage-4 and stage-6 materials. The magnetic ordering wave-vector is exactly the same for both dopings. By applying a high magnetic field of up to 14.5 T, we measure the field-induced change in the SDW Bragg peak intensity. The field-induced enhancement of the SDW signal follows the prediction of the recently proposed model of competing superconducting and magnetic orders in doped La_2CuO_4. The $H \ln H$ field dependence of the SDW signal demonstrates the quantitative agreement between experiment and theory.

Acknowledgments

We have benefited from useful discussions with E. Demler, S. Sachdev, P. A. Lee and Y. J. Uemura. This work has been supported at MIT by the MRSEC Program of the National Science foundation under Award No. DMR 02-13282, by NSF under Awards No. DMR 0071256 and DMR 99-71264. Work at the University of Toronto is part of the Canadian Institute for Advanced Research and is supported by the Natural Science and Engineering Research Council of Canada. We acknowledge the support of the National Institute of Standards and Technology, U.S. Department of Commerce, and the Berlin Neutron Scattering Center, Hahn-Meitner Institute, Berlin, in providing the neutron facilities used in this work.

[1] H. Yoshizawa *et al.* J. Phys. Soc. Jpn. **57**, 3686 (1988); R. Birgeneau et al., Phys. Rev. B **39** 2868 (1989); S. W. Cheong, G. Aeppli, T. E. Mason, H. Mook, S. M. Hayden, P. C. Canfield, Z. Fisk, K. N. Clausen, and J. L. Martinez, Phys. Rev. Lett. **67**, 1791 (1991).

[2] K. Yamada, C. H. Lee, K. Kurahashi, J. Wada, S. Wakimoto, S. Ueki, H. Kimura, Y. Endoh, S. Hosoya, G. Shirane, R. J. Birgeneau, M. Greven, M. A. Kastner, Y. J. Kim, Phys. Rev. B **57**, 6165 (1998).

[3] J. M. Tranquada, B. J. Sternlieb, J. D. Axe, Y. Nakamura, S. Uchida, Nature **375**, 561 (1995); N. Ichikawa, S. Uchida, J. M. Tranquada, T. Niemoller, P. M. Gehring, S.-H. Lee, and J. R. Schneider, Phys. Rev. Lett. **85**, 1738 (2000).

[4] H. Kimura, K. Hirota, H. Matsushita, K. Yamada, Y. Endoh, S.-H. Lee, C. F. Majkrzak, R. W. Erwin, G. Shirane, M. Greven, Y. S. Lee, M. A. Kastner, R. J. Birgeneau Phys. Rev. B **59**, 6517 (1999).

[5] Y. S. Lee, R. J. Birgeneau, M. A. Kastner, Y. Endoh, S. Wakimoto, K. Yamada, R. W. Erwin, S.-H. Lee, G. Shirane, Phys. Rev. B **60**, 3643 (1999).

[6] S. Wakimoto *et al.*, Phys. Rev. B. **61**, 3699 (2002).

[7] B. Khaykovich, Y. S. Lee, R. W. Erwin, S.-H. Lee, S. Wakimoto, K. J. Thomas, M. A. Kastner, and R. J.Birgeneau, Phys. Rev. B **66**, 014528 (2002).

[8] S. Katano, M. Sato, K. Yamada, T. Suzuki, and T. Fukase, Phys. Rev. B **62**, R14677 (2000).

[9] B. Lake, G. Aeppli, K. N. Clausen, D. F. McMorrow, K. Lefmann, N. E. Hussey, N. Mangkorntong, M. Nohara, H. Takagi, T. E. Mason, A. Schroder, Science **291**, 1759 (2001).

[10] B. Lake, H. M. Ronnow, N. B. Christensen, G. Aeppli, K. Lefmann, D. F. McMorrow, P. Vorderwisch, P. Smeibidl, N. Mangkorntong, T. Sasegawa, M. Nohara, H. Takagi, T. E. Mason, Nature **415**, 299 (2002).

[11] E. Demler, S. Sachdev, and Y. Zhang, Phys. Rev. Lett **87**, 067202 (2001); Y. Zhang, E. Demler, S. Sachdev, Phys. Rev. B **66**, 094501 (2002).

[12] S.-C. Zhang, Science **275**, 1089 (1997); J.-P. Hu and S.-C. Zhang, preprint cond-mat/0108273 (2001).

[13] S. Kivelson *et. al.*, preprint cond-mat/0205228.

[14] J. Zaanen and O. Gunnarsson, Phys. Rev. B **40**, 7391 (1989); J. Zaanen, Physica C, **317**, 217 (1999).

[15] M. Matsuda, M. Fujita, K. Yamada, R. J. Birgeneau, Y. Endoh, G. Shirane, Phys. Rev. B **66**, 174508 (2002).

[16] A. Savici, Y. Fudamoto, I. M. Gat, M. I. Larkin, Y. J. Uemura, K. M. Kojima, Y. S. Lee, M. A. Kastner, R. J. Birgeneau, Physica B **289-290**, 338 (2000).

[17] A. Savici, Y. Fudamoto, I. M. Gat, T. Ito, M. I. Larkin, Y. J. Uemura, G. M. Luke, K. M. Kojima, Y. S. Lee, M. A. Kastner, R. J. Birgeneau, K. Yamada, Phys. Rev. B **66**, 014524 (2002).

[18] B. O. Wells, Y. S. Lee, M. A. Kastner, R. J. Christianson, R. J. Birgeneau, K. Yamada, Y. Endoh, G. Shirane, Science **277**, 1067 (1997).

[19] Y. S. Lee, M. A. Kastner, R. J. Birgeneau, unpublished.

[20] R. Gilardi *et al.*, Phys. Rev. Lett. 88, 217003(2002).